

Bismuth – Indium – Antimony

Tamara Velikanova, Mikhail Turchanin, Hans Leo Lukas

Introduction

Scientific interest in phase relationships in the Bi–In–Sb system is mainly due to two reasons. The first one is a potential application for long wavelength infrared detector materials. The second one is the development of Pb free solders.

The first systematic and most extensive studies on the Bi–In–Sb phase diagram are the three consecutive works of Peretti [1958Per, 1960Per, 1961Per] in which a number of vertical sections were determined using DTA and X-ray diffraction. [1979Ufi] presented the InSb–In₂Bi vertical section. The Bi solubility limit in InSb was investigated by [1964Kos, 1972Jou, 1977Lat, 1979Ufi, 1980Zil1, 1981Lan, 2000Moh].

Experimental works of [1979Ufi, 2000Moh, 2000Dix, 2000Iwa] were devoted to studies of growth and structural properties of single crystals. Data on the growth and structural properties of thin films were obtained by [1978Zil, 1980Cad, 1980Zil1, 1980Zil2, 1997Lee1, 1999Wag, 1999Gao, 2001Osz]. The structure of rapidly quenched solid solutions of InSb–InBi alloys has been studied by [1991She].

Thermodynamic properties of liquid ternary alloys were investigated by [1976Vec, 1978Pre, 1982Erm, 1986Gor, 1997Kam]. Thermal effects of phase transitions have been studied by [1988Evg].

These and some more experimental works are summarized in Table 1.

A calculation of the phase diagram by the Calphad method has been carried out by [2002Cui].

Binary Systems

For the Bi–In, Bi–Sb and In–Sb systems the assessments of [Mas2] were accepted. Thermodynamic data sets of [2002Cui] for the Bi–In system, of [1992Feu] for Bi–Sb and of [1994Ans] for In–Sb were used to calculate diagrams and the reaction scheme presented in this assessment.

Solid Phases

No ternary compound has been reported. Table 2 summarizes data for the unary and binary phases. Negligible solubilities of the third component are found in all binary phases except InSb [1964Kos, 1958Per, 1960Per, 1961Per, 1977Lat, 1979Ufi, 1980Zil1, 2000Moh].

From the solid solutions Al_xIn_{1–x}Sb, Ga_xIn_{1–x}Sb and InAs_xSb_{1–x} [2005Sch, 2005Luk, 2005Mis] it is known, that the homogenization of InSb solid solutions is very slow and even above the melting temperature of pure InSb needs more than 1000 h to be effective. Thus the measured composition in most cases is the frozen in equilibrium composition during growth conditions. For liquid phase epitaxy or single crystal synthesis by the methods of Bridgman or Czochralski these conditions depend mainly on the composition of the melt. The temperature of growth is a range just below the liquidus temperature of this composition. [1972Jou] varied the InBi content in InSb–InBi melts up to 70 mol% and from grown single crystals determined the solidus curve of InSb_{1–x}Bi_x (Fig. 2) along this section. [2000Moh] by the same method measured a solidus curve of similar shape but about 1 mol% larger solubility of InBi. [2000Dix] reported a higher value of $x = 0.065$ for the composition of a single crystal grown from a melt with 20 mol% InSb + 80 mol% InBi. Three other papers [1977Lat, 1979Ufi, 1981Lan] reported slightly lower x values than [1972Jou] for solid solutions grown from melts of the section InSb–InBi. These authors measured also samples grown from melts of the sections InSb–Bi and InSb–In₂Bi and reported lower Bi contents for the first one, but slightly higher Bi contents for the second one. The generally accepted assumption, that the homogeneity range of InSb_{1–x}Bi_x is practically restricted to Sb–Bi exchange thermodynamically postulates the highest Bi solubility to be in the InSb–InBi section. In the dataset of [2002Cui] the homogeneity range of InSb_{1–x}Bi_x is neglected. Considering the possibility of Bi substitution on the Sb sublattice of this phase and adding a parameter ${}^{\circ}L^{\beta}_{\text{In:Bi}} = 5300 - 5T + 0.5({}^{\circ}G^{\text{(In)}}_{\text{In}} + {}^{\circ}G^{\alpha}_{\text{Bi}})$ J·mol^{–1} to the dataset the calculation reproduces well the solidus line $x = f(T)$ of InSb_{1–x}Bi_x given by [1972Jou].

The lattice parameter variation of the $\text{InSb}_{1-x}\text{Bi}_x$ solid solution up to $x = 0.017$ is given in Fig. 1 according to the measurements of [1972Jou]. It can be represented as $a = 647.9 + 16x$ pm. These results correlate well with data of [2000Moh] where the lattice parameter was found to increase from 647.8 to 648.1 pm in the range $x = 0$ to $x = 0.02$.

Metastable single-crystal epitaxial $\text{InSb}_{1-x}\text{Bi}_x$ solid films with $x = 0.12$ (6 at.% Bi) were obtained by sputtering from independently controlled InSb and Bi targets [1980Zil1, 1980Zil2, 1980Cad]. The authors believe that these maximum values obtained in their experiments along the InSb–InBi section do not belong to a fundamental limit of the solid solubility.

Quasibinary Systems

The two vertical sections InSb–InBi and InSb– In_2Bi are likely to be quasibinary ones because the three compounds InSb, InBi and In_2Bi melt congruently. Indeed [1958Per, 1960Per, 1961Per, 1972Jou, 1979Ufi] reported the sections InSb–InBi and InSb– In_2Bi to be quasibinary systems of eutectic type (degenerated to the compositions of InBi and In_2Bi), respectively.

No temperature maximum or minimum was found along the monovariant line of the liquid phase in the $L \rightleftharpoons \beta + \alpha$ three-phase equilibrium [1958Per, 1960Per]. Thus the vertical section InSb–Bi is not a quasibinary system, which is easily understandable as in the binary systems the liquidus temperature increases monotonically from Bi towards Sb, but decreases monotonically from Bi towards the Bi + InBi eutectic. Calculations using the dataset of [2002Cui] confirm the quasibinary degenerated eutectic character of the two sections InSb–InBi and InSb– In_2Bi (Figs. 2 and 3). In Fig. 3 the boundary of β is not exactly in the plane of section, but at 50 at.% In. The line in the diagram is the projection into the section plane along constant Bi content. The section InSb–Bi is clearly not quasibinary.

Invariant Equilibria

Invariant equilibria calculated from the dataset of [2002Cui] are given in Table 3. In E_1 , U_1 , U_2 , E_2 , and E_3 the liquid phase participates. In the publication [2002Cui] the authors reported the reactions E_1 and E_2 as U type reactions, the compositions given, however, show clearly the liquids to be located inside the triangles of the three solid phases and thus the reactions clearly are ternary eutectics. The temperatures of U_1 and E_3 reported by [2002Cui] do not exactly fit with the recalculated ones. Due to a ternary extension of Raoult's law the difference between the binary Bi–In three-phase equilibrium temperatures and the ternary four-phase temperatures are strongly related to the Sb mole fractions of liquid in the four-phase equilibria. To show these differences the temperatures in Table 3 and Fig. 4 are given with two digits after the point. With the assumption of zero solubility of Sb in (In), δ , ϵ phases coexisting in the solid-phase equilibrium D_1 this equilibrium is totally degenerated and exactly equals to the binary eutectoid $\epsilon \rightleftharpoons \delta + (\text{In})$ with the β phase being in equilibrium but not participating in the reaction. In reality it may be either below (E type) or above (U type) the binary three-phase reaction depending, if the solubility of Sb in ϵ is greater or less than the mean of the Sb solubilities in δ and (In), respectively. The calculated reaction scheme is given in Fig. 4. The calculated equilibrium temperatures are in good agreement with the experimental ones measured by [1960Per, 1961Per].

Liquidus and Solidus Surfaces

A liquidus surface projection of the Bi–In–Sb is given in Fig. 5, calculated from the dataset of [2002Cui] showing liquidus isotherms at temperature intervals of 50°C. The liquidus temperatures increase significantly with increasing Sb concentration whereas the solidus temperatures only slightly are suppressed, they contain the invariant equilibria summarized in Table 2. A liquidus surface projection drawn by [1960Per] shows the univariant curve $L + \alpha + \beta$ going exactly into the Bi corner, which is thermodynamically very unlikely. As [2002Cui] showed, the experimental points of [1960Per] fit equally well with the calculated vertical sections, meaning that this unlikely feature of the liquidus surface is not supported by the experimental data.

The solidus surface of the Bi–In–Sb system in Fig. 6 is calculated using the dataset of [2002Cui] with the additional parameter ${}^{\circ}L_{\text{In:Bi}}^{\beta}$ mentioned above.

Isothermal Sections

Below the solidus temperature the β phase ($\text{InSb}_{1-x}\text{Bi}_x$) is in equilibrium with all other solid phases. The corresponding isothermal sections can be constructed by connecting all boundaries of the binary phase diagrams by straight lines with the β phase. This is demonstrated in Fig. 7 by the calculated isothermal section at 75°C. Isothermal sections above the lowest solidus temperature can be constructed similarly using additionally the corresponding liquidus isotherm shown in Fig. 5. Only the α corner of the three-phase equilibrium $L + \alpha + \beta$ has to be extra calculated. It is somewhat more Sb rich than the corresponding solidus temperature of the binary Bi–Sb system. This is demonstrated by the calculated isothermal sections at 300 and 400°C in Figs. 8 and 9, respectively.

Temperature – Composition Sections

Seventeen vertical sections were measured by Peretti [1958Per, 1960Per, 1961Per]. Twelve of them were calculated by [2002Cui] and compared with Peretti's experimental points. The fit with the experimental points is very good, although the drawings of Peretti contain some unlikely or even incorrect features. Only the calculated temperatures of secondary crystallization of the (Bi,Sb) solid solution (α phase) are significantly higher than the measured ones. This may be due to segregation as the first parts of the primarily crystallizing solid solution contain nearly pure Sb and do not equilibrate during the following crystallization. Thus the experimental points belong to secondary crystallization starting in a melt depleted by Sb at a lower temperature, whereas the calculation gives equilibrium temperatures where the $L + \alpha / L + \alpha + \beta$ boundary passes the initial composition of the sample. In Figs. 10 and 11 two calculated vertical sections are shown as examples.

Thermodynamics

The enthalpy of mixing of Bi–In–Sb melts was determined by quantitative thermal analysis at 632°C for five sections with constant In/Bi ratios of 16/1, 2/1, 1/1, 1/2, and 1/9 by [1976Vec]. The error of the determination was estimated to be about 5%. The obtained results are represented graphically in Fig. 12 by isoenthalpy lines. Bi–In–Sb liquid alloys are characterized by positive and negative deviations from ideality. The maximum enthalpy of mixing $-4.99 \pm 0.20 \text{ kJ}\cdot\text{mol}^{-1}$ corresponds to a ternary composition with $x_{\text{In}} = 0.441$ and $x_{\text{Bi}} = 0.059$.

The enthalpy of mixing along the InSb–Bi section was determined by [1978Pre] at 612°C using a high temperature calorimeter. The derived enthalpies of mixing were reported with reference not to the pure liquid elements as in Fig. 12, but referenced to the pure binary liquid InSb and liquid pure Bi, Fig. 13. They show a positive deviation from ideality with a maximum at about $0.56 \text{ kJ}\cdot\text{mol}^{-1}$ near $x_{\text{Bi}} = 0.6$. The authors compared their results with calculations using a Redlich–Kister description as well as an approach to the associated solution model.

The thermodynamic activity of bismuth in dilute InSb–Bi liquid alloys with $x_{\text{Bi}} < 0.014$ has been determined by emf measurements (immersion method) at 678°C by [1982Erm]. For bismuth concentrations up to 1 at.% the deviation from ideality is negative. A transition to positive deviations from Raoult's law occurs at bismuth concentrations above 1 at.%.

The partial Gibbs energies of indium in liquid and heterogeneous mixtures were obtained by the emf method [1986Gor] for three sections with constant Bi:Sb ratios of 2:1, 1:1 and 1:2 in the temperature interval 497 to 527°C. From the temperature dependencies of the measured emf values partial enthalpies of mixing of In were derived. The results (Fig. 14) were used for calculation of the integral properties in the whole concentration range and of the liquidus surface.

Thermal effects accompanied with the crystallization of liquid alloys belonging to the InSb–InBi and InSb–In₂Bi sections were studied by quantitative thermal analysis by [1988Evg]. Their results are shown in Table 4. The concentration dependence of these thermal effects show regions near InSb in both the

InSb–InBi and InSb–In₂Bi sections in which these thermal effects are larger than the heat of fusion of InSb. This is in accordance with the positive enthalpy of mixing shown in Fig. 13.

Thermodynamic activities of indium in liquid alloys was studied between 613 and 906°C by [1997Kam] using the emf method with zirconia solid electrolyte. These investigations were carried out at fifteen alloys along the three sections In–Bi_{0.8}Sb_{0.2}, In–Bi_{0.5}Sb_{0.5}, and In–Bi_{0.2}Sb_{0.8}. The results are shown in Fig. 15.

The mixing enthalpy and Gibbs energy of liquid alloys were estimated by [1991Pri] in the framework of their own empirical model.

The enthalpies of mixing measured by [1978Pre], the activities of In in liquid from [1997Kam] and the partial enthalpy of mixing of In in liquid from [1986Gor] were used by [2002Cui] for a thermodynamic assessment of the system. The corresponding curves calculated from the assessed thermodynamic dataset are shown in Figs. 13 to 15. As the figures show, this thermodynamic dataset reproduces well the measured thermochemical quantities of liquid in the ternary system. As was outlined in the previous chapters the thermodynamic description proposed by [2002Cui] fits also well with most experimental data of phase relations in the system. This thermodynamic assessment can be improved by considering substitution of Sb by Bi in the β phase and modeling the ternary solubility of this phase, which was neglected by [2002Cui]. As already pointed out above in “solid phases” the sublattice model In(Bi,Sb) with a single parameter $^{\circ}L_{\text{In,Bi}}^{\beta} = 5300 - 5T + 0.5(^{\circ}G_{\text{In}}^{\beta} + ^{\circ}G_{\text{Bi}}^{\alpha}) \text{ J}\cdot\text{mol}^{-1}$ added, the assessed dataset enables good reproduction of the measurements of Bi solubility in β by [1972Jou].

Notes on Materials Properties and Applications

In the last years increasing efforts have been made to search for suitable Pb free solders. Since Bi, In and Sb are important elements for the development of Pb free solders, the Bi–In–Sb system is included in the present volume considering its potential technical perspective for solder applications.

Table 5 summarizes the available experimental works devoted to the study of physical properties of InSb_{1–x}Bi_x bulk alloys and thin films. Main emphasis in investigation of materials properties of Bi–In–Sb alloys was given to the InSb_{1–x}Bi_x phase. This material is very interesting as it is a semiconductor InSb modified by InBi with semi-metal behaviour. Hence the band-gap energy can be varied over a wide range. Consequently narrow-gap semiconducting compounds can be obtained, which are of highest interest as promising materials for photoelectronic devices operating in the long wavelength infrared range (7.4 to 16 μm) [1997Lee1, 1997Lee2, 1998Lee, 2000Iwa]. The limited equilibrium solubility of Bi in InSb is the main obstacle in the growth of InSb_{1–x}Bi_x alloys with optimal electronic properties. The liquid phase epitaxy method (LPE) provides a maximum Bi alloy content of $x = 0.01$ to 0.025 with $E_g \approx 0.1 \text{ eV}$ [1979Ufi, 1981Lan, 1997Akc] depending on the growth temperature, which is somewhat below the liquidus temperature of the selected liquid composition.

Supersaturated thin films can be obtained by sputtering [1978Zil, 1980Zil1, 1980Zil2, 1980Cad] with Bi contents up to 6 at.% (x up to 0.12), by low-pressure metalorganic chemical vapor deposition (LP-MOCVD) [1997Lee1, 1997Lee2, 1998Lee, 1999Wag] with x up to 0.058, by quenching of liquid with a rate of about $10^6 \text{ K}\cdot\text{s}^{-1}$ [1991She] ($x = 0.02$ to 0.04), or by flash evaporation [2001Osz] ($x = 0.02$). An increase of the electron concentration and a decrease of their mobility was observed with increasing Bi content of the solid solution. Figures 16 and 17 show these properties, measured by [1997Lee2] at 77 and 300 K, as functions of the Bi content. The metastable single-phase films show very good thermal stability. After annealing up to 120 h at temperatures below 229°C films with $x = 0.12$ remained single phase [1980Zil2]. Annealing 12 h at 266°C resulted in precipitation of Bi (α phase). After additional annealing for 12 h at 304°C finally the X-ray pattern of the InBi phase was observed. For films of lower supersaturation the annealing temperatures for decompositions into $\alpha + \beta$ or $\alpha + \beta + \gamma$ increase as shown in Fig. 18.

The band gap E_g was calculated ab initio by the empirical pseudopotential method [1998Vy, 1999Dei] as function of the Bi content ($2x$ in InSb_{1–x}Bi_x) at three different temperatures, 0, 77 and 300 K. It is shown in Fig. 19a, the corresponding temperature coefficient in Fig. 19b. The results agree well with data from optical absorption experiments of [1969Jea]. Ab initio calculations of [1973Jea] gave a smaller decrease of the bandgap vs Bi content of 67% of that shown in Fig. 19a. [2000Dix] reported a bandgap of 113 meV at room temperature and a composition of $x = 0.0654$ (3.27 at.% Bi), which is higher than the values mentioned

before. Other measured properties of $\text{InSb}_{1-x}\text{Bi}_x$ solid solutions are Hall coefficient [1969Jea, 1991She, 2000Dix], electric conductivity [1991She, 2000Dix] and microhardness (Fig. 20) [1977Lat, 2000Moh].

References

- [1958Per] Peretti, E.A., "The System InSb-InBi", *Trans. Metall. Soc. AIME*, **212**(1), 79 (1958) (Experimental, Phase Diagram, 3)
- [1960Per] Peretti, E.A., "Constitution Studies of the Antimony and Bismuth-Rich Portions of the Sb-Bi-In System", *Trans. ASM*, **52**, 1046-1058 (1960) (Experimental, Phase Diagram, 7)
- [1961Per] Peretti, E.A., "Constitution Studies of the Indium-Rich Portion of the System Antimony-Bismuth-Indium", *Trans. ASM*, **54**, 12-19 (1961) (Experimental, Phase Diagram, Phase Relations, 6)
- [1964Kos] Kostur, I. L., Psaryev, V. I., "Solubility of Certain Elements in InSb and CdSb and Their Effects on their Effect on the Physical Properties", *Ukrain. Fiz. Zhur.*, **9**(8), 900-907 (1964) (Crys. Structure, Electr. Prop., Experimental, Mechan. Prop., Phase Relations, Thermodyn., 6)
- [1969Jea] Jean-Louis, A.M., Hamon, C., "Properties of the $\text{InSb}_{1-x}\text{Bi}_x$ Alloys" (in French), *Phys. Status Solidi*, **34**, 329-340 (1969) (Calculation, Electr. Prop., Electronic Structure, Experimental, 11)
- [1972Jou] Joukoff, B., Jean-Louis, A.M., "Growth of $\text{InSb}_{1-x}\text{Bi}_x$ Single Crystals by Czochralski Method", *J. Cryst. Growth*, **12**(2), 169-172 (1972) (Crys. Structure, Experimental, Phase Relations, 3)
- [1973Jea] Jean-Louis, A.M., Duraffourg, G., "Properties of the $\text{InSb}_{1-x}\text{Bi}_x$ Alloys. III. Theoretical Estimation of the Forbidden Band" (in French), *Phys. Status Solidi B*, **59**, 495-503 (1973) (Calculation, Crys. Structure, Electronic Structure, 21)
- [1976Vec] Vecher, A.A., Mechkovskii, L.A., Rubenchik, G.B., Savitskii, A.A., Skoropanov, A.S., "The Enthalpies of Formation of Indium-Bismuth-Antimony Melts", *Russ. J. Phys. Chem. (Engl. Transl.)*, **50**(11), 1759-1760 (1976), translated from *Zh. Fiz. Khim.*, **50**, 2956-2958 (1976) (Experimental, Phase Relations, Thermodyn., 11)
- [1977Lat] Latypov, Z.M., Saveliev, V.P., Averyanov, I.S., Faizullina, N.R., Prikhodtsev, M.N., "Investigation of the Region of Solid Solutions Based on InSb in the In-Sb-Bi System", *Izv. Akad. Nauk SSSR, Neorg. Mater.*, **13**, 910-911 (1977) (Experimental, Phase Relations, Mechan. Prop., 0)
- [1978Pre] Predel, B., Gerdes, F., "Thermodynamic of the Liquid Alloys of the InSb-Pd and InSb-Bi Systems", *J. Less-Common Met.*, **59**, 153-164 (1978) (Experimental, Phase Relations, Thermodyn., 10)
- [1978Zil] Zilko, J.L., Greene, J.E., "Growth of Metastable $\text{InSb}_{1-x}\text{Bi}_x$ Thin Films by Multitarget Sputtering", *Appl. Phys. Lett.*, **33**(3), 254-256 (1978) (Experimental, Interface Phenomena, Phys. Prop., 14)
- [1979Ger] Gerdes, F., Predel, B., "Thermodynamic Properties of the Liquid Alloys of the InSb-Bi, GaSb-Bi and AlSb-Bi Systems" (in German), *J. Less-Common Met.*, **65**(1), 41-49 (1979) (Experimental, Thermodyn., 11)
- [1979Ufi] Ufimtsev, V.B., Zinov'ev, V.G., Raukman, M.R., "Heterogeneous Equilibria in the System In-Sb-Bi, and Liquid-Phase Epitaxy of InSb-Based Solid Solutions", *Inorg. Mater. (Engl. Trans.)*, **15**(10), 1371-1374 (1979), translated from *Izv. Akad. Nauk SSSR, Neorg. Mater.*, **15**(10), 1740-1743 (1979) (Experimental, Phase Diagram, Phase Relations, Phys. Prop., 11)
- [1980Cad] Cadien, K.C., Zilko, J.L., Eltoukhy, A.H., Greene, J.E., "Growth of Single-Crystal Metastable $\text{InSb}_{1-x}\text{Bi}_x$ and $(\text{GaSb})_{1-x}\text{Ge}_x$ Semiconducting Films", *J. Vac. Sci. Technol.*, **17**(1), 441-444 (1980) (Electr. Prop., Experimental, Phase Relations, 14)

- [1980Zil1] Zilko, J.L., Greene, J.E., "Growth and Phase Stability of Epitaxial Metastable $\text{InSb}_{1-x}\text{Bi}_x$ Films on GaAs. I. Crystal Growth", *J. Appl. Phys.*, **51**(3), 1549-1559 (1980) (Crys. Structure, Electr. Prop., Experimental, Optical Prop., 32)
- [1980Zil2] Zilko, J.L., Greene, J.E., "Growth and Phase Stability of Epitaxial Metastable $\text{InSb}_{1-x}\text{Bi}_x$ Films on GaAs. II. Phase Stability", *J. Appl. Phys.*, **51**(3), 1560-1564 (1980) (Electronic Structure, Experimental, 10)
- [1981Lan] Lantsov, A.F., Akuchrin, R.Kh., Zinov'ev, V.G., "Distribution of Bismuth in Epitaxial Layers of InSb / Bi ", *Inorg. Mater. (Engl. Trans.)*, **17**, 1146-1148 (1981), translated from *Izv. Akad. Nauk SSSR, Neorg. Mater.*, **17**(9) 1550-1553 (1981) (Experimental, Transport Phenomena, 7)
- [1982Erm] Ermakov, A.V., Egorkin, V.V., Ufimtsev, V.B., "Study of the Thermodynamic Properties of Dilute In-Sb-Bi Melts by the Immersion Method", *Russ. J. Phys. Chem. (Engl. Transl.)*, **56**(6), 942-944 (1982) (Experimental, Thermodyn., 12)
- [1986Gor] Goryacheva, V.I., Pashin, S.F., Geiderikh, V.A., "Thermodynamic Properties and Liquidus of the Indium-Bismuth-Antimony System", *Vestn. Mosk. Univ., Ser. 2: Khim.*, **26**(2), 142-150 (1985) (Experimental, Phase Diagram, Thermodyn.) as quoted by [2002Cui]
- [1988Evg] Evgen'ev, S.B., "Thermal Effects of Phase Transitions in the Ga-Sb-Bi and In-Sb-Bi Systems", *Inorg. Mater. (Engl. Trans.)*, **24**, 454-457 (1988), translated from *Izv. Akad. Nauk SSSR, Neorg. Mater.*, **24**(4), 546-549 (1988) (Experimental, Phase Relations, Thermodyn., 6)
- [1991Pri] Prikhod'ko, E.V., Garmash, L.I., "Effect of the Charged State of the Components on the Thermodynamic Properties of Metallic Melts", *Russ. Metall. (Engl. Transl.)*, **6**, 209-213 (1991), translated from *Izv. Akad. Nauk SSSR, Met.*, (6), 215-219 (1991) (Calculations, Thermodyn., 2)
- [1991She] Shepelevich, V.G., "Structure and Electrical Properties of Rapidly Quenched InSb Foils and of Solid Solutions of the System InSb-InBi ", *Inorg. Mater. (Engl. Trans.)*, **27**(12), 2150-2152 (1991), translated from *Izv. Akad. Nauk SSSR, Neorg. Mater.*, **27**(12), 2505-2507 (1991) (Crys. Structure, Electr. Prop., Experimental, 7)
- [1992Feu] Feutelais, Y., Morgant, G., Didry, J.R., Schnitter J., "Thermodynamic Evaluation of the System Bismuth-Antimony", *Calphad*, **16**(2), 111-119 (1992) (Calculation, Phase Diagram, Thermodyn., 47)
- [1994Ans] Ansara, I., Chatillon, C., Lukas, H.L., Nishizawa, T., Ohtani, H., Ishida, K., Hillert, M., Sundman, B., Argent, B.B., Watson, A., Chart, T. G., Anderson, T., "A Binary Database for III-V Compound Semiconductor Systems", *Calphad*, **18**(2), 172-222 (1994) (Calculation, Phase Diagram, Thermodyn.)
- [1997Akc] Akchurin, R.Kh., Komarov, D.V., "Formation of Multilayer Strained-Layer Heterostructures by Liquid Epitaxy. II. Simulation of the Fabrication of Heterostructures Based on Indium-Arsenic-Antimony-Bismuth Solid Solutions", *Tech. Phys.*, **42**(7), 762-768 (1997) (Crys. Structure, Experimental, Thermodyn., 11)
- [1997Lee1] Lee, J.J., Kim, J.D., Razeghi, M., "Long-Wavelength Infrared Photodetectors Based on InSbBi Grown on GaAs Substrates", *Appl. Phys. Lett.*, **71**(16), 2298-2300 (1997) (Electr. Prop., Experimental, Optical Prop., 14)
- [1997Lee2] Lee, J.J., Kim, J.D., Razeghi, M., "Growth and Characterization of InSbBi for Long Wavelength Infrared Photodetectors", *Appl. Phys. Lett.*, **70**(24), 3266-3268 (1997) (Electronic Structure, Experimental, Optical Prop., 16)
- [1997Kam] Kameda, K., Yamaguchi, K., Kon T., "Activity of Indium in Molten In-Pb-Ag and In-Bi-Sb Alloys Measured by an EMF Method Using a Zirconia Electrolyte", *Nippon Kinzoku Gakkaishi*, **61**(5), 444-448 (1997) (Experimental, Thermodyn.)
- [1998Lee] Lee, J.J., Kim, J.D., Razeghi, M., "Room Temperature Operation of 8-12 μm InSbBi Infrared Photodetectors on GaAs Substrates", *Appl. Phys. Lett.*, **73**(5), 602-604 (1998) (Electr. Prop., Experimental, 10)

- [1998Vyk] Vyklyuk, J.I., Deibuk, V.G., "The Band Structure and Electron Density of $\text{InSb}_{1-x}\text{Bi}_x$ Solid Solutions", *Acta Phys. Pol. A*, **94**(3), 611-616 (1998) (Electronic Structure, Experimental, 14)
- [1999Dei] Deibuk, V. G., Viklyuk, Ya. I., Rarenko, I. M., "Calculating the Band Structure of $\text{InSb}_{1-x}\text{Bi}_x$ Solid Solution", *Semicond.*, **33**(3), 293-296 (1999) (Calculation, Electronic Structure, 14)
- [1999Gao] Gao, Y.Z., Yamaguchi, T., "Liquid Phase Epitaxial Growth and Properties of InSbBi Films Grown from In, Bi and Sn Solutions", *Cryst. Res. Technol.*, **34**(3), 285-292 (1999) (Electr. Prop., Experimental, Morphology, Optical Prop., 8)
- [1999Wag] Wagener, M.C., Kroon, R.E., Botha, J.R., Leitch, A.W.R., "Analysis of Secondary Phases in InSbBi Thin Films", *Physica B*, **273-274**, 919-922 (1999) (Crys. Structure, Experimental, 9)
- [2000Dix] Dixit, V.K., Rodrigues, B.V., Bhat, H.L., "Growth of $\text{InSb}_{(1-x)}\text{Bi}_x$ Crystals by Rotatory Bridgman Method and Their Characterization", *J. Cryst. Growth*, **217**, 40-46 (2000) (Crys. Structure, Electr. Prop., Experimental, Magn. Prop., 6)
- [2000Iwa] Iwanowski, R.J., Heinonen, M.H., Raczynska, J., Fronc, K., "XPS Analysis of Surface Compositional Changes in $\text{InSb}_{1-x}\text{Bi}_x$ (111) Due to Low-Energy Ar^+ Ion Bombardment", *Appl. Surf. Sci.*, **153**, 193-199 (2000) (Electronic Structure, Interface Phenomena, Experimental, 26)
- [2000Moh] Mohan, P., Babu, S.M., Santhanaraghavan, P., Ramasamy, P., "Growth, Phase Analysis and Mechanical Properties of $\text{InSb}_{1-x}\text{Bi}_x$ Crystals", *Mater. Chem. Phys.*, **66**, 17-21 (2000) (Experimental, Mechan. Prop., Phase Relations, 14)
- [2001Osz] Oszwaldowski, M., Berus, T., Szade, J., Jozwiak, K., Olejniczak, I., Konarski, P., "Structural Properties of InSbBi and InSbAsBi Thin Films Prepared by the Flash-Evaporation Method", *Cryst. Res. Technol.*, **36**(8-10), 1155-1171 (2001) (Crys. Structure, Electr. Prop., Experimental, Optical Prop., 28)
- [2002Cui] Cui, Y., Ishihara, S., Liu, X.J., Ohnuma, I., Kainuma, R., Ohtani, H., Ishida, K., "Thermodynamic Calculation of Phase Diagram in the Bi-In-Sb Ternary System", *Mater. Trans., JIM*, **43**(8), 1879-1886 (2002) (Calculation, Phase Diagram, Phase Relations, Thermodyn., 26)
- [2005Sch] Schmid-Fetzer, R., Lukas, H.L., "Aluminium-Indium-Antimony", in Landolt-Boernstein, Numerical Data and Functional Relationships in Science and Technology (New Series). Group IV: Physical Chemistry. Ed. W. Martienssen, "Ternary Alloy Systems. Phase Diagrams, Crystallographic and Thermodynamic Data", Vol. 11C1, Effenberg, G., Ilyenko, S., (Eds.), Springer-Verlag, Berlin, Heidelberg, 144-153, (2005) (Phase Relations, Phase Diagram, Thermodyn., Crys. Structure, Assessment, 24)
- [2005Luk] Lukas, H.L., "Gallium-Indium-Antimony", in Landolt-Boernstein, Numerical Data and Functional Relationships in Science and Technology (New Series). Group IV: Physical Chemistry. Ed. W. Martienssen, "Ternary Alloy Systems. Phase Diagrams, Crystallographic and Thermodynamic Data", Vol. 11C1, Effenberg, G., Ilyenko, S., (Eds.), Springer-Verlag, Berlin, Heidelberg, 412-426, (2005) (Phase Relations, Phase Diagram, Thermodyn., Crys. Structure, Assessment, 68)
- [2005Mis] Misra, S., Anderson, T., Ansara, I., Ivanchenko, V., Lakiza, S., "Arsenic-Indium-Antimony", in Landolt-Boernstein, Numerical Data and Functional Relationships in Science and Technology (New Series). Group IV: Physical Chemistry. Ed. W. Martienssen, "Ternary Alloy Systems. Phase Diagrams, Crystallographic and Thermodynamic Data", Vol. 11C1, Effenberg, G., Ilyenko, S., (Eds.), Springer-Verlag, Berlin, Heidelberg, 227-241, (2005) (Phase Relations, Phase Diagram, Thermodyn., Crys. Structure, Assessment, 85)

Table 1: Investigations of the Bi–In–Sb Phase Relations, Structures and Thermodynamics

Reference	Method/Experimental Technique	Temperature/Composition/Phase Range Studied
[1958Per]	Thermal analysis, X-ray analysis, optical microscopy	InSb–InBi, 100–600°C
[1960Per]	Thermal analysis, X-ray analysis, optical microscopy	8 vertical sections in Bi–InBi–InSb–Sb part of system, 100–600°C
[1961Per]	Thermal analysis, X-ray analysis, optical microscopy	8 vertical sections in InBi–InSb–In part of system, 50–600°C
[1964Kos]	X-ray analysis	$\text{In}_x(\text{InSb})_y\text{Bi}_z$ as-cast ingots and single crystals, $x = 0.7632\text{--}0.9208$, $y = 0.0765\text{--}0.2258$, $z = 0.0027\text{--}0.0110$
[1972Jou]	Differential thermal analysis, X-ray analysis, liquid phase epitaxy	single crystal samples $\text{InSb}_{1-x}\text{Bi}_x$, $x = 0\text{--}0.026$
[1976Vec]	Quantitative thermographic analysis	Enthalpy of mixing of liquid, at 632°C in the whole composition triangle
[1977Lat]	X-ray analysis, microhardness measurements	InSb–InBi, InSb–In ₂ Bi and InSb–Bi, 90–99.75 mol.% InSb
[1978Pre] [1979Ger]	High temperature calorimetry	InSb–Bi, 612°C
[1978Zil]	Thin film growth by multi target sputtering	metastable supersaturated $\text{InSb}_{1-x}\text{Bi}_x$ ($x \leq 0.12$) solid solutions
[1979Ufi]	DTA, liquid phase epitaxy	InSb–(In ₂ Bi, InBi or Bi), 300–500°C
[1979Ufi]	Differential thermal analysis, local X-ray-spectral analysis	InSb–InBi, InSb–In ₂ Bi and InSb–Bi, 100–600°C
[1980Cad]	Wavelength dispersive energy analysis, scanning transmission electron microscopy	polycrystalline metastable $\text{InSb}_{1-x}\text{Bi}_x$ films, $x = 0.07\text{--}0.12$, 200–500°C
[1980Zil1]	Wavelength dispersive energy analysis, X-ray analysis	Single-crystal metastable $\text{InSb}_{1-x}\text{Bi}_x$ films, $x = 0.02\text{--}0.12$, 200–500°C
[1980Zil2]	X-ray analysis	metastable $\text{InSb}_{1-x}\text{Bi}_x$ films, $x = 0\text{--}0.12$ bulk alloys $\text{InSb}_{1-x}\text{Bi}_x$, $x < 0.031$, 90°C
[1981Lan]	Radioisotopic tracer method, local X-ray-spectral analysis	InSb–InBi, InSb–In ₂ Bi InSb–Bi epitaxial layers, $x_{\text{Bi}} < 0.015$, 220–450°C
[1982Erm]	Emf immersion method	a_{Bi} , InSb–Bi, $x_{\text{Bi}} < 0.014$, 678°C
[1986Gor]	Emf salt electrolyte method	sections at Bi/Sb ratios 2/1 and 1/1 at 497°C, 1/2 at 527°C
[1988Evg]	Quantitative differential thermal analysis	$\Delta_{\text{cr}}H$, InSb–InBi, InSb–In ₂ Bi
[1991She]	X-ray analysis	InSb–InBi rapidly quenched foils, 100–300°C

Reference	Method/Experimental Technique	Temperature/Composition/Phase Range Studied
[1997Kam]	Emf solid electrolyte method	a_{In} , sections In–Bi _{0.8} Sb _{0.2} , In–Bi _{0.5} Sb _{0.5} , In–Bi _{0.2} Sb _{0.8} , 613–906°C
[1997Lee1] [1997Lee2]	Energy dispersive X-ray analysis, X-ray analysis of thin films grown by low pressure metalorganic chemical vapor deposition	InSb _{1–x} Bi _x films, $x = 0$ –0.058, 70–300 K
[1999Gao]	Optical microscopy, electron-probe micro analysis of films grown by liquid phase epitaxy	InSb _{1–x} Bi _x epilayers, ($0.01 < x < 0.14$)
[1999Wag]	Scanning electron microscopy, cross-sectional transmission electron microscopy, X-ray analysis of films grown by metalorganic vapor deposition	InSb _{1–x} Bi _x films, 455°C
[2000Dix]	Energy-dispersive X-ray analysis, X-ray analysis, differential scanning calorimetry, infrared spectroscopy. Bridgman single crystal synthesis	InSb _{1–x} Bi _x single crystals, $x = 0.0654$
[2000Iwa]	X-ray photoelectron spectroscopy	single crystalline InSb _{1–x} Bi _x epitaxial layer, $x = 0.005$, 190–310°C
[2000Moh]	Differential thermal analysis, optical microscopy, X-ray analysis, scanning electron microscopy	InSb _{1–x} Bi _x , $x = 0$ –0.02, 50–700°C
[2001Osz]	X-ray analysis, scanning electron microscopy, X-ray microanalysis, secondary ion mass spectrometry. Metastable thin films prepared by flash evaporation	InSb _{1–x} Bi _x films, $x \leq 0.2$, 285–715°C

Table 2: Crystallographic Data of Solid Phases

Phase/ Temperature Range [°C]	Pearson Symbol/ Space Group/ Prototype	Lattice Parameters [pm]	Comments/References
α , Bi _{1–x} Sb _x	$hR6$ $R\bar{3}m$		$0 < x < 1$, [Mas2]
(Bi) < 271.442	As	$a = 454.613$ $c = 1186.152$	pure Bi, 25°C [V-C2]
(Sb) < 630.755		$a = 430.84$ $c = 1127.4$	pure Sb, 25°C [V-C2]
(In), In _{1–x} Bi _x < 156.634	$tI2$ $I4/mmm$ In	$a = 325.3$ $c = 497.70$	$0 < x < 0.08$ [Mas2] pure In, 25°C [Mas2]

Phase/ Temperature Range [°C]	Pearson Symbol/ Space Group/ Prototype	Lattice Parameters [pm]	Comments/References
γ , InBi < 110.0	<i>tP4</i> <i>P4/nmm</i> PbO	$a = 501.5$ $c = 478.8$	[Mas2] [V-C2]
χ , In ₅ Bi ₃ < 88.9	<i>tI32</i> <i>I4/mcm</i> Cr ₃ B ₅	$a = 854.4$ $c = 1268$	62.2 to 62.66 at.% In [Mas2] [V-C2]
δ , In ₂ Bi < 89.5	<i>hP6</i> <i>P6₃/mmc</i> Ni ₂ In	$a = 549.6$ $c = 657.9$	66.8 to 67.7 at.% In [Mas2] [V-C2]
ϵ , In _{1-x} Bi _x 93.5 - 49	<i>tI2</i> <i>I4/mmm</i> In	$a = 347.2$ $c = 449.5$	$0.08 \leq x \leq 0.12$ [Mas2] 90 at.% In at 70°C [V-C2]
β , InSb _{1-x} Bi _x < 525.7	<i>cF8</i> <i>F43m</i> ZnS	$a = 647.9$	$0 < x < 0.026$ [1972Jou] at $x = 0$ [1972Jou]

Table 3: Invariant Equilibria

Reaction	T [°C]	Type	Phase	Composition (at.%)		
				In	Bi	Sb
$L \rightleftharpoons \beta + \gamma$	109.76	e ₃ (max)	L	49.992	49.992	0.016
$L \rightleftharpoons \alpha + \beta + \gamma$	109.19	E ₁	L	47.477	52.509	0.014
$L + (\text{In}) \rightleftharpoons \beta + \epsilon$	93.37	U ₁	L	82.518	17.445	0.037
$L + \gamma \rightleftharpoons \beta + \chi$	88.84	U ₂	L	64.744	35.244	0.012
$L \rightleftharpoons \beta + \delta$	88.16	e ₅ (max)	L	66.658	33.329	0.012
$L \rightleftharpoons \beta + \delta + \chi$	88.09	E ₂	L	65.888	34.100	0.012
$L \rightleftharpoons \beta + \epsilon + \delta$	72.54	E ₃	L	77.778	22.210	0.012
$\epsilon \rightleftharpoons \delta + \beta + (\text{In})$	49.07	D ₁	-	-	-	-

Table 4: Thermodynamic Data of Reaction or Transformation

Reaction or Transformation	T [°C]	Quantity, per mol of compound [kJ·mol ⁻¹]	Comments
$L \rightarrow \text{InSb}$	525.7	$\Delta_{\text{cr}}H = 47.0 \pm 6.1$	quantitative differential thermal analysis, [1988Evg]
$L \rightarrow x\text{InSb} + (1-x)\text{InBi}$	T_L-T_S	$\Delta_{\text{cr}}H = 56.4 \pm 7.3$	$x = 0.99$
	T_L-T_S	$\Delta_{\text{cr}}H = 37.8 \pm 4.9$	$x = 0.95$
	T_L-T_S	$\Delta_{\text{cr}}H = 38.8 \pm 5.0$	$x = 0.80$
	T_L-T_S	$\Delta_{\text{cr}}H = 26.2 \pm 3.4$	$x = 0.60$
	T_L-T_S	$\Delta_{\text{cr}}H = 22.5 \pm 2.9$	$x = 0.38$
	T_L-T_S	$\Delta_{\text{cr}}H = 31.2 \pm 4.0$	$x = 0.20$
	T_L-T_S	$\Delta_{\text{cr}}H = 31.4 \pm 4.1$	$x = 0.05$
	$T_e = 110$	$\Delta_{\text{cr}}H = 10.0 \pm 1.3$	Eutectic
$L \rightarrow x\text{InSb} + (1-x)\text{In}_2\text{Bi}$	T_L-T_S	$\Delta_{\text{cr}}H = 37.8 \pm 4.9$	$x = 0.95$
	T_L-T_S	$\Delta_{\text{cr}}H = 38.8 \pm 5.0$	$x = 0.80$
	T_L-T_S	$\Delta_{\text{cr}}H = 26.2 \pm 3.4$	$x = 0.60$
	T_L-T_S	$\Delta_{\text{cr}}H = 22.5 \pm 2.9$	$x = 0.38$
	T_L-T_S	$\Delta_{\text{cr}}H = 31.2 \pm 4.0$	$x = 0.20$
	T_L-T_S	$\Delta_{\text{cr}}H = 31.4 \pm 4.1$	$x = 0.05$
	$T_e = 90$	$\Delta_{\text{cr}}H = 10.0 \pm 1.3$	Eutectic

Table 5: Investigations of the $\text{InSb}_{1-x}\text{Bi}_x$ Materials Properties

Reference	Method/Experimental Technique	Type of Property
[1964Kos]	Compensating method In magnetic field 6800 e	Thermo emf Hall effect
[1969Jea]	In magnetic field	Electrical conductivity Hall effect
[1980Zil2]	Infrared spectrometry Van der Pauw technique	Absorption coefficient Hall effect
[1997Lee1, 1997Lee2]	Van der Pauw technique Infrared spectrometry X-ray spectrometry Scanning electron microscopy Nomarski differential interference contrast microscopy	Hall effect Photoconductive spectral response

Reference	Method/Experimental Technique	Type of Property
[1998Lee]	Infrared spectrometry	Spectral voltage response
	Van der Pauw technique	Hall effect
	X-ray spectrometry	
	Energy dispersive X-ray analysis	
[2000Dix]	Infrared spectrometry	Absorption coefficient
	Van der Pauw technique	Hall effect
[2000Moh]	Vickers microhardness experiments	Microhardness

Fig. 1: Bi–In–Sb.
Composition
dependence of the
lattice parameter of
 $\text{InSb}_{1-x}\text{Bi}_x$ solid
solutions

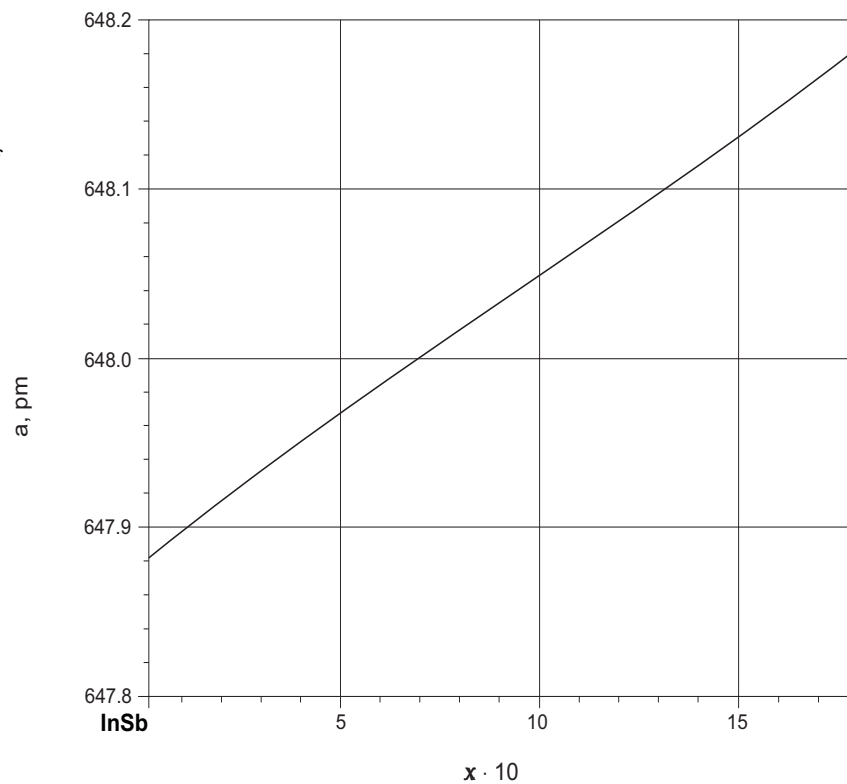


Fig. 2: Bi-In-Sb.
Calculated
quasibinary system
InBi-InSb

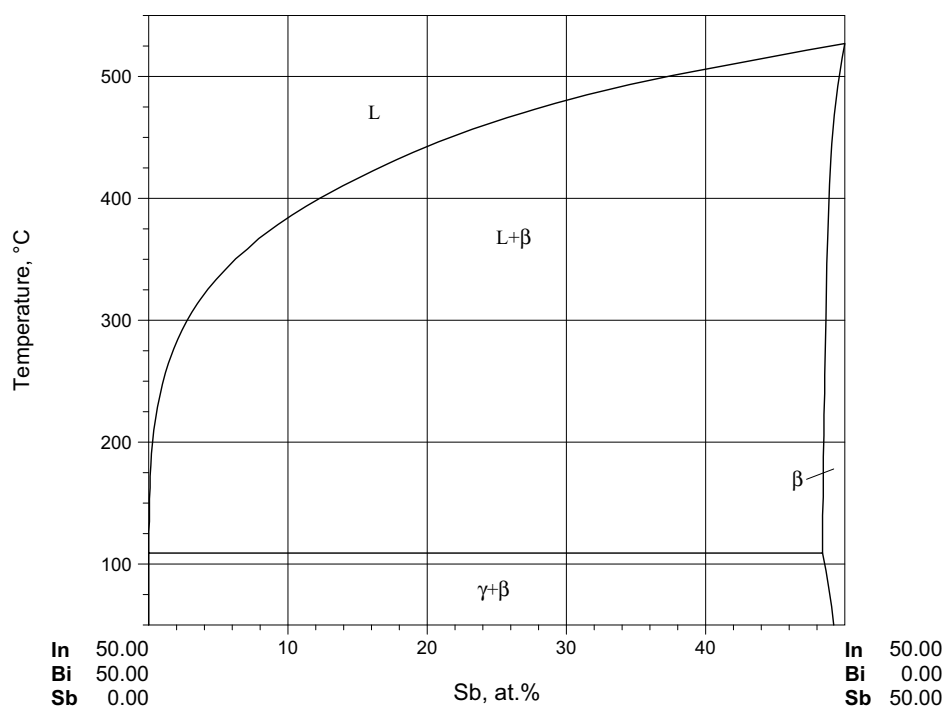
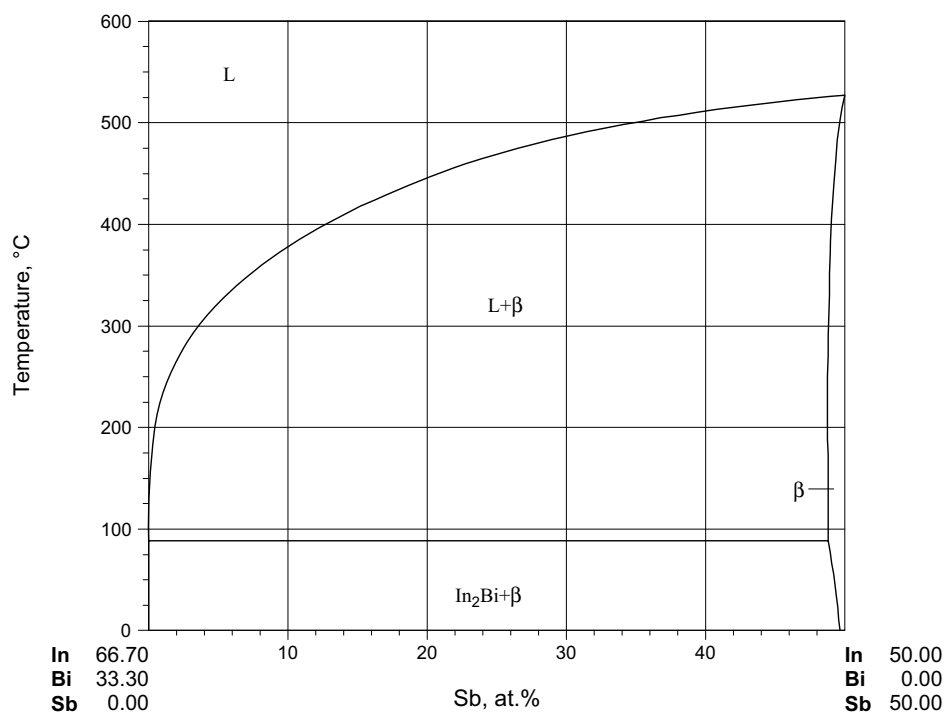


Fig. 3: Bi-In-Sb.
Calculated
quasibinary system
In₂Bi-InSb



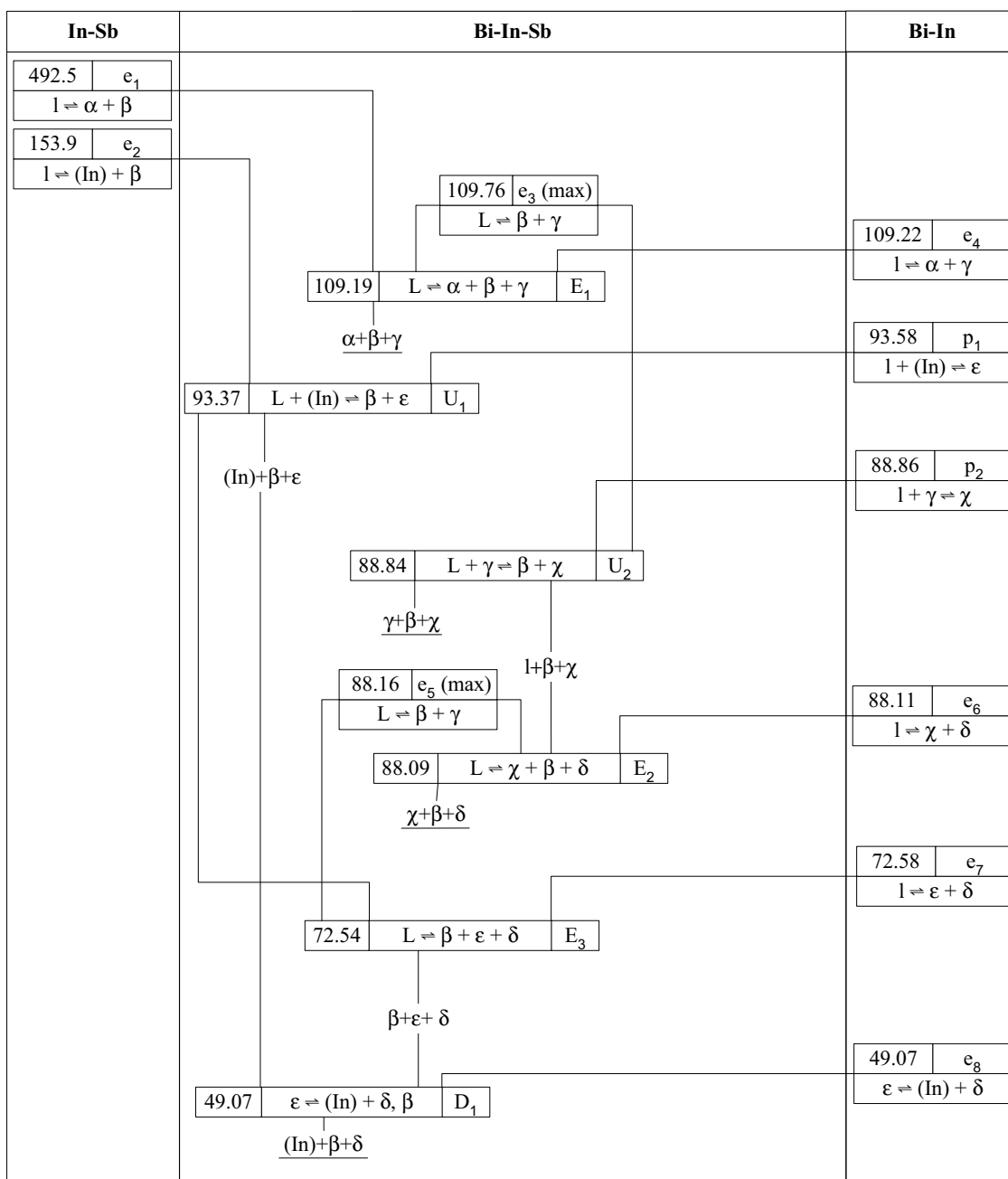


Fig. 4: Bi-In-Sb. Reaction scheme

Fig. 5: Bi-In-Sb.
Calculated liquidus
surface projection

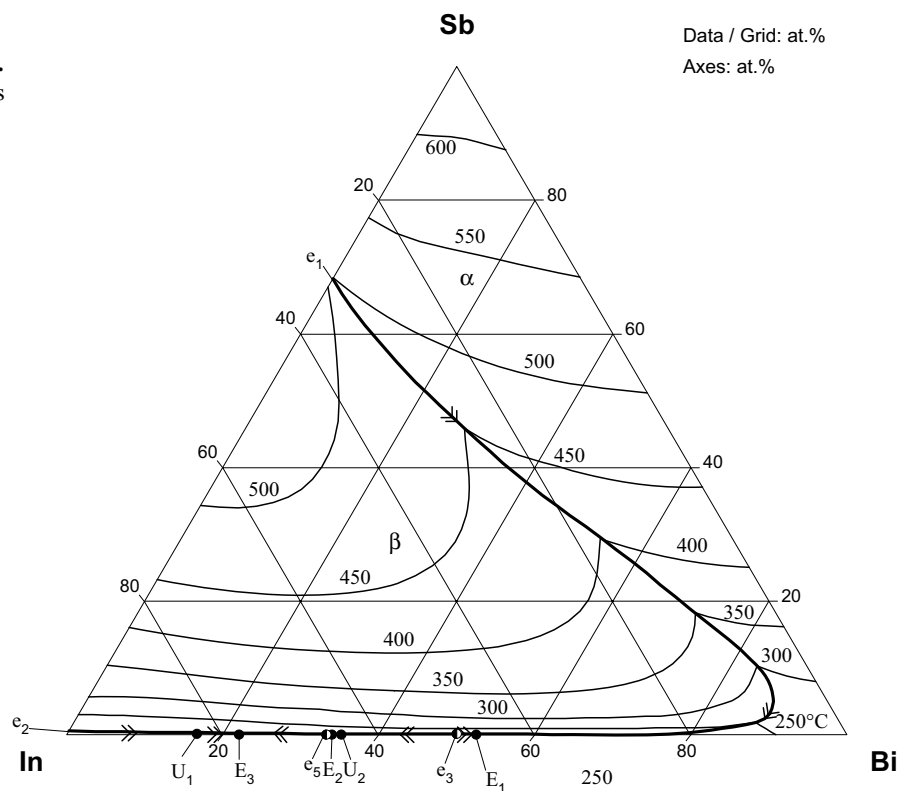


Fig. 6: Bi-In-Sb.
Calculated solidus
surface

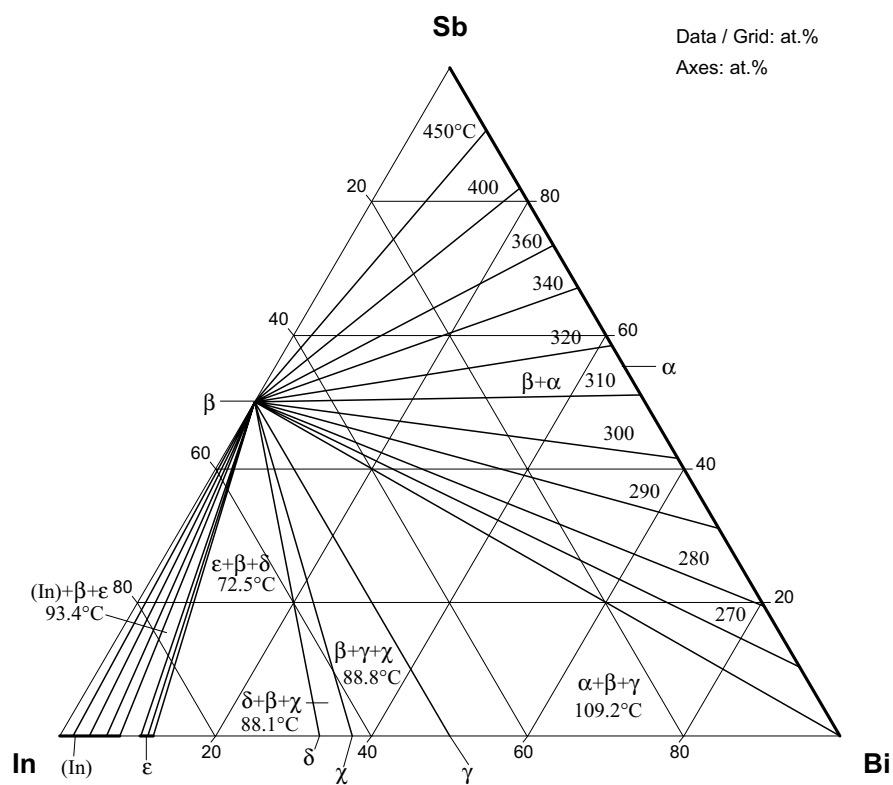


Fig. 7: Bi-In-Sb.
Calculated isothermal
section at 75°C

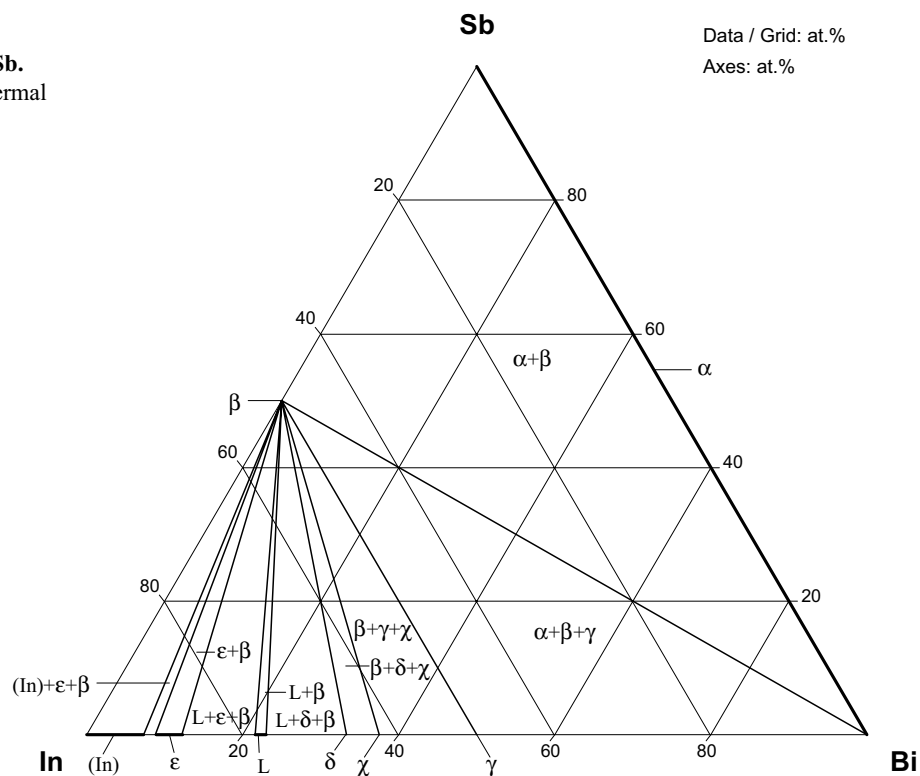


Fig. 8: Bi-In-Sb.
Calculated isothermal
section at 300°C

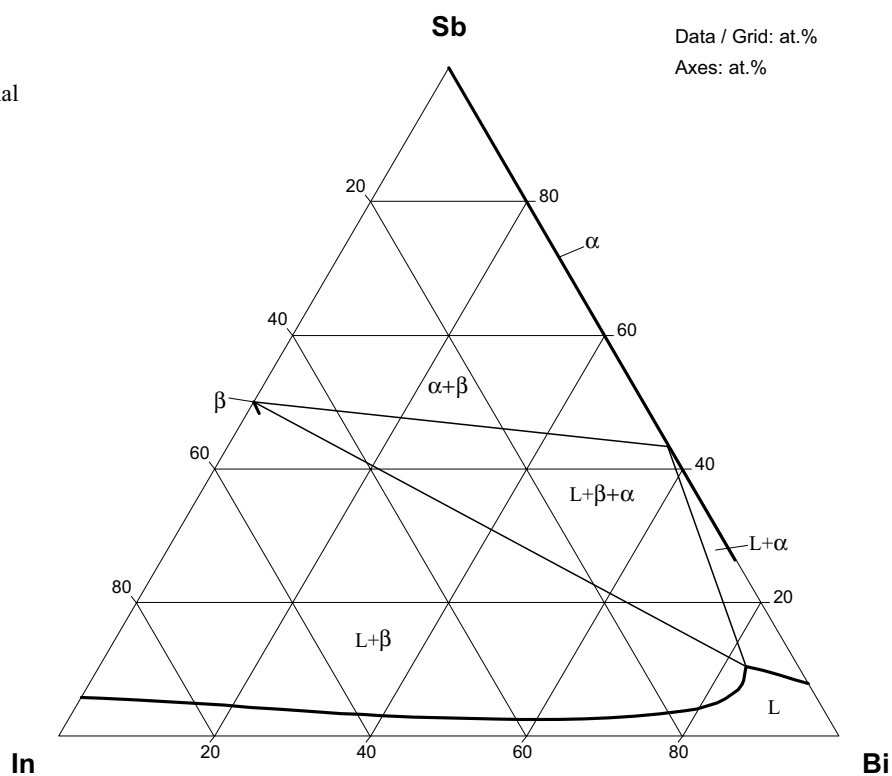


Fig. 9: Bi-In-Sb.
Calculated isothermal
section at 400°C

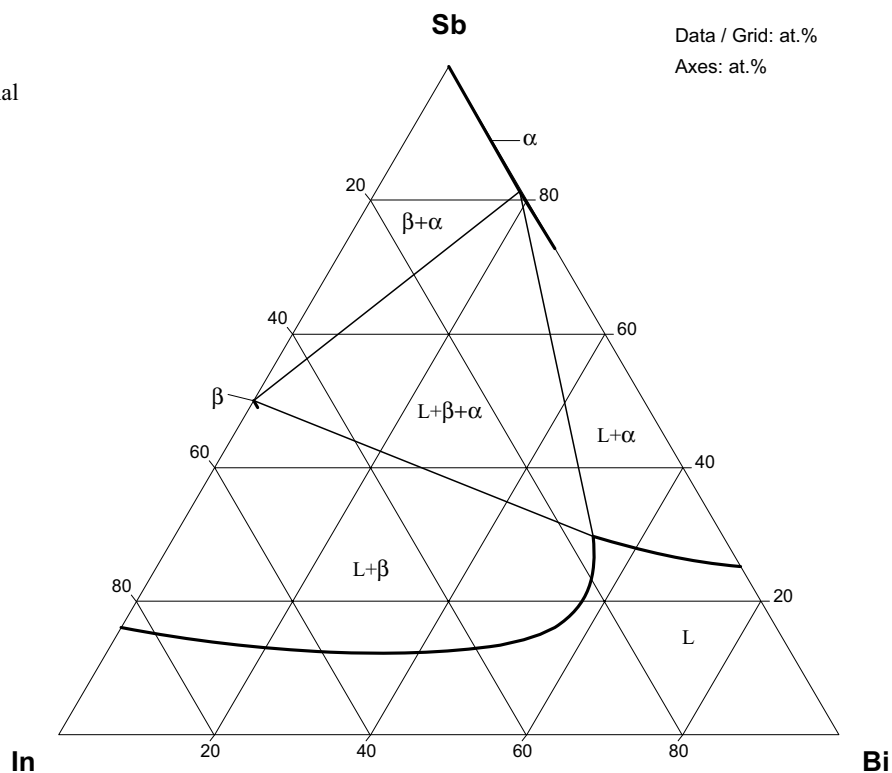


Fig. 10: Bi-In-Sb.
Calculated vertical
section at 10 at.% Sb

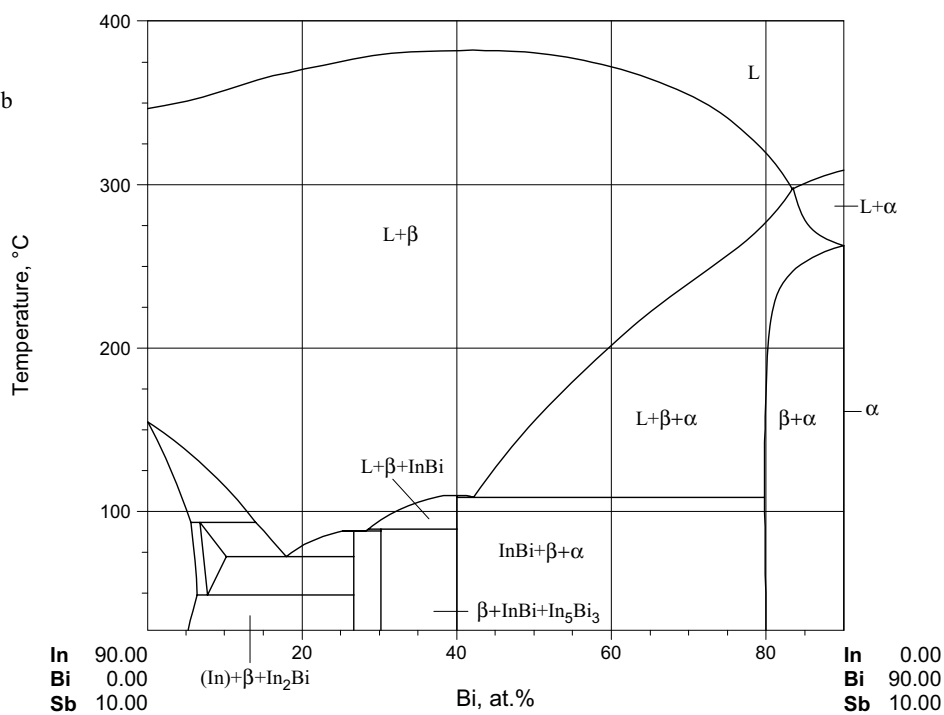


Fig. 11: Bi-In-Sb.
Calculated vertical
section InBi-Sb

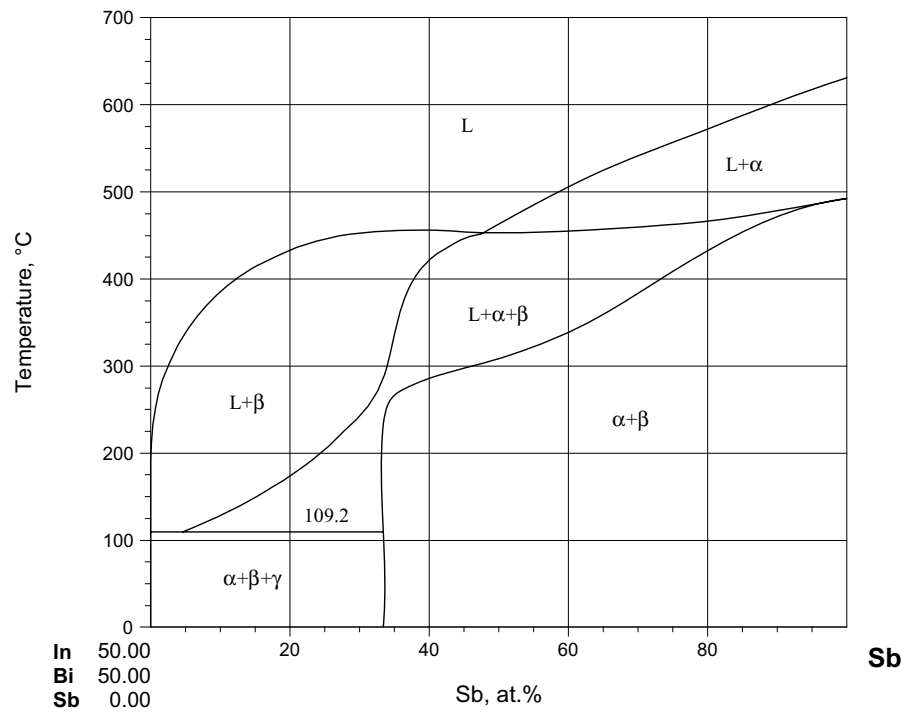


Fig. 12: Bi-In-Sb.
Mixing enthalpies of
Bi-In-Sb liquid alloys
at 632°C ($\text{kJ}\cdot\text{mol}^{-1}$)

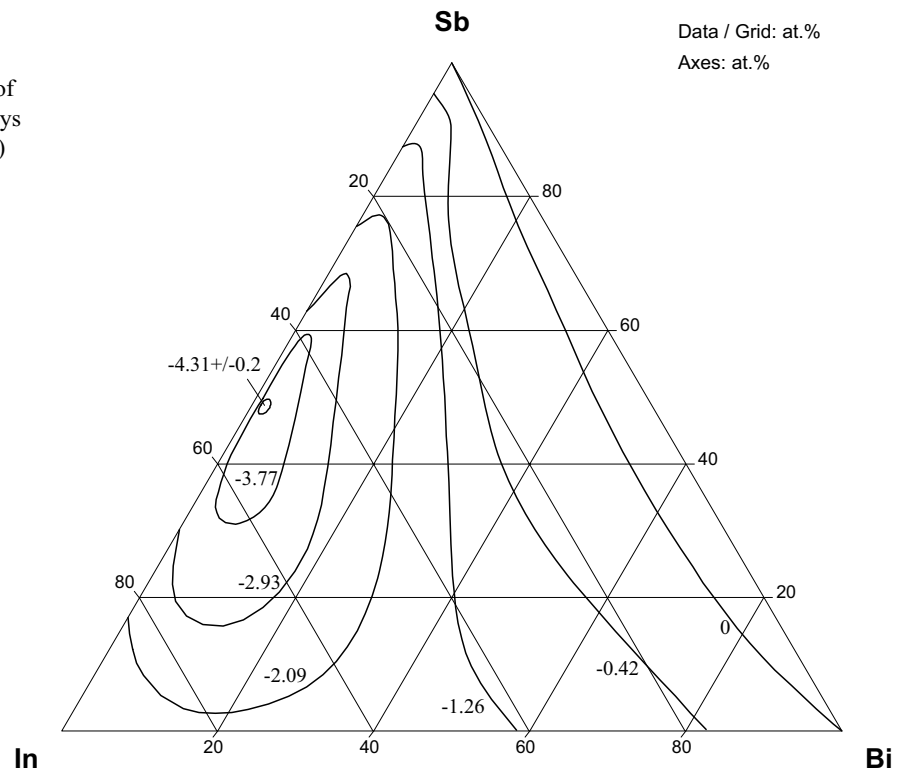


Fig. 13: Bi-In-Sb.
Enthalpy of mixing
along the InSb-Bi
section at 612°C:
Triangles -
experimental results
of [1978Pre], solid
line - calculated by
[2002Cui]

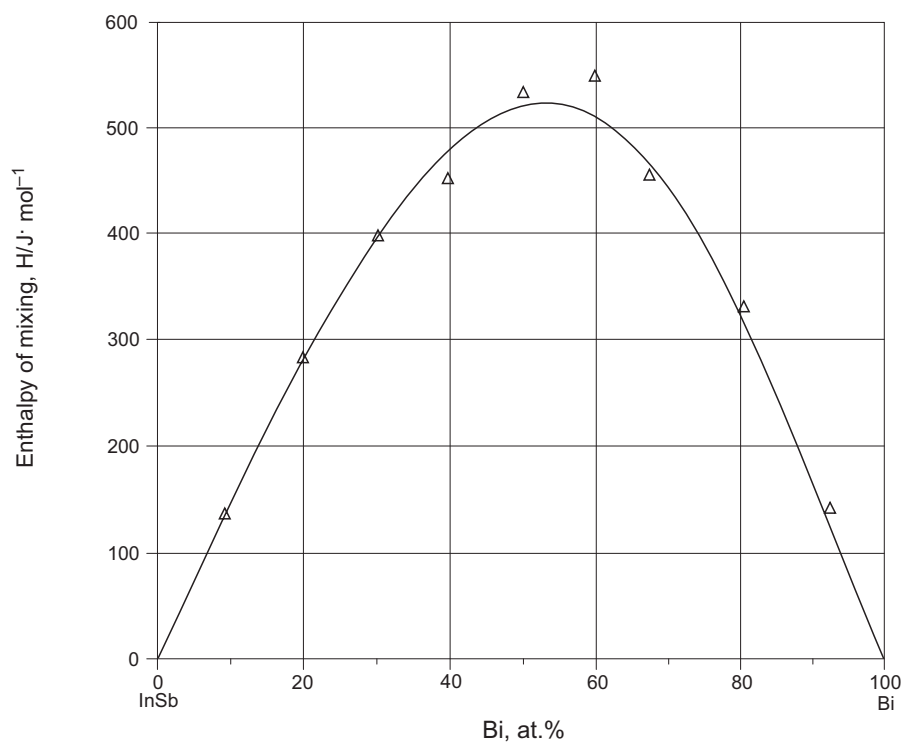


Fig. 14: Bi-In-Sb.
Partial enthalpy of
mixing of In in liquid
alloys along sections
with constant Bi/Sb
ratios: symbols -
experimental results
[1986Gor] (triangles -
Bi/Sb = 1/2, 497°C;
circles - Bi/Sb = 1/1,
497°C; crosses -
Bi/Sb = 1/2, 527°C;
lines: calculated by
[2002Cui] at same
temperatures (solid -
Bi/Sb = 2/1, dashed -
Bi/Sb = 1/1, dots -
Bi/Sb = 1/2)

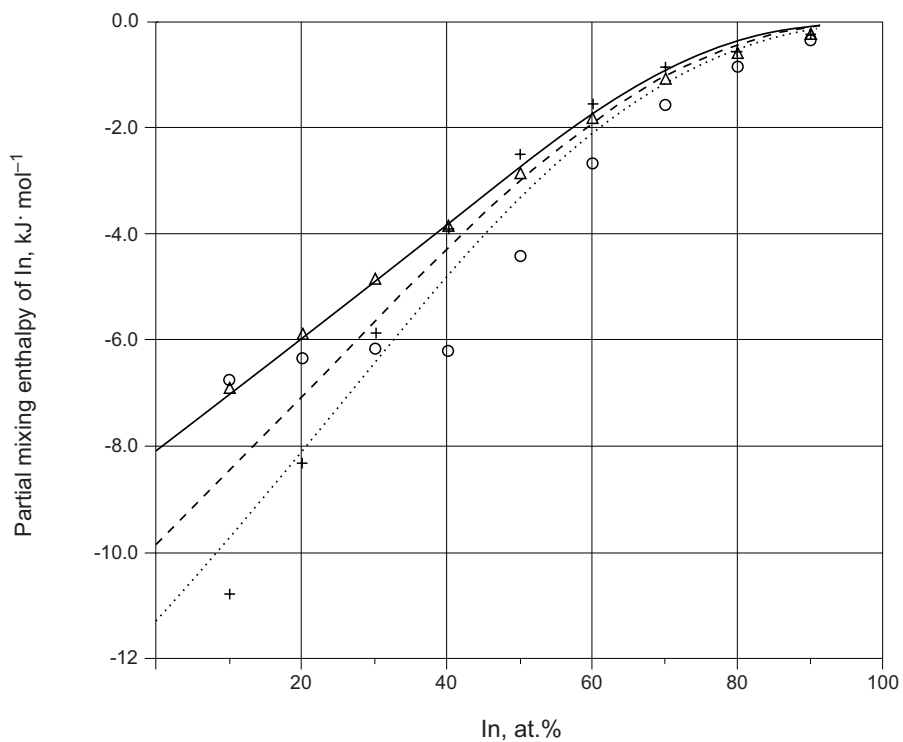
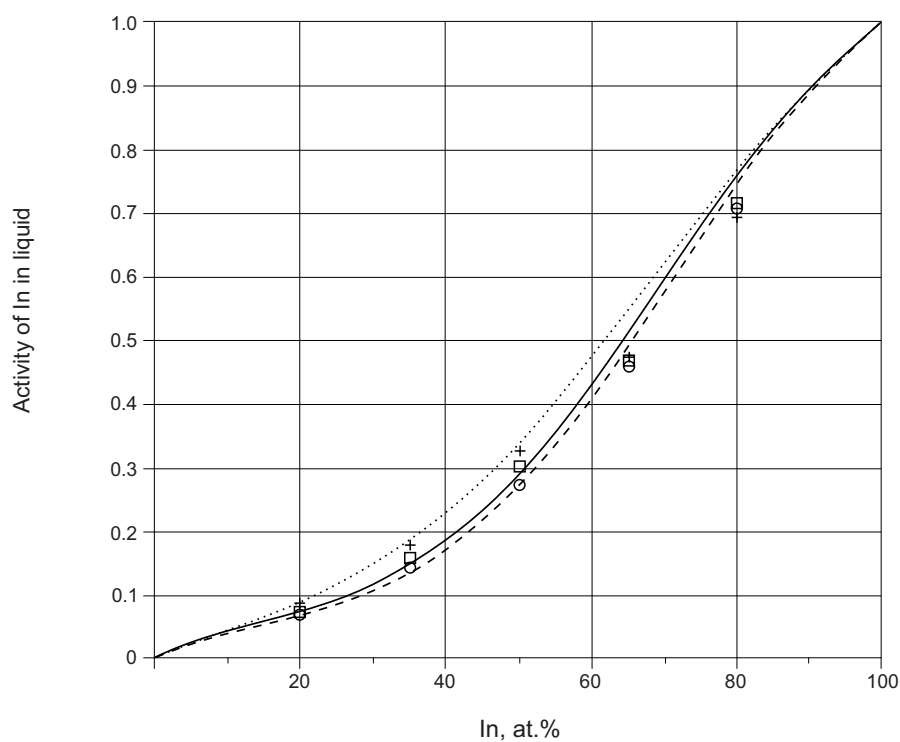


Fig. 15: Bi-In-Sb.

Activity of In in liquid alloys at 727°C along sections with constant Bi/Sb ratios:

symbols - experimental results [1997Kam] (crosses - In-Bi_{0.8}Sb_{0.2}, squares - InBi_{0.5}Sb_{0.5}, circles - In-Bi_{0.2}Sb_{0.8}); lines - calculated by [2002Cui] (dots - In-Bi_{0.8}Sb_{0.2}, solid - In-Bi_{0.5}Sb_{0.5}, dashed - In-Bi_{0.2}Sb_{0.8})

**Fig. 16: Bi-In-Sb.**

Electron concentration of InSb_{1-x}Bi_x vs Bi concentration at 77 and 300 K

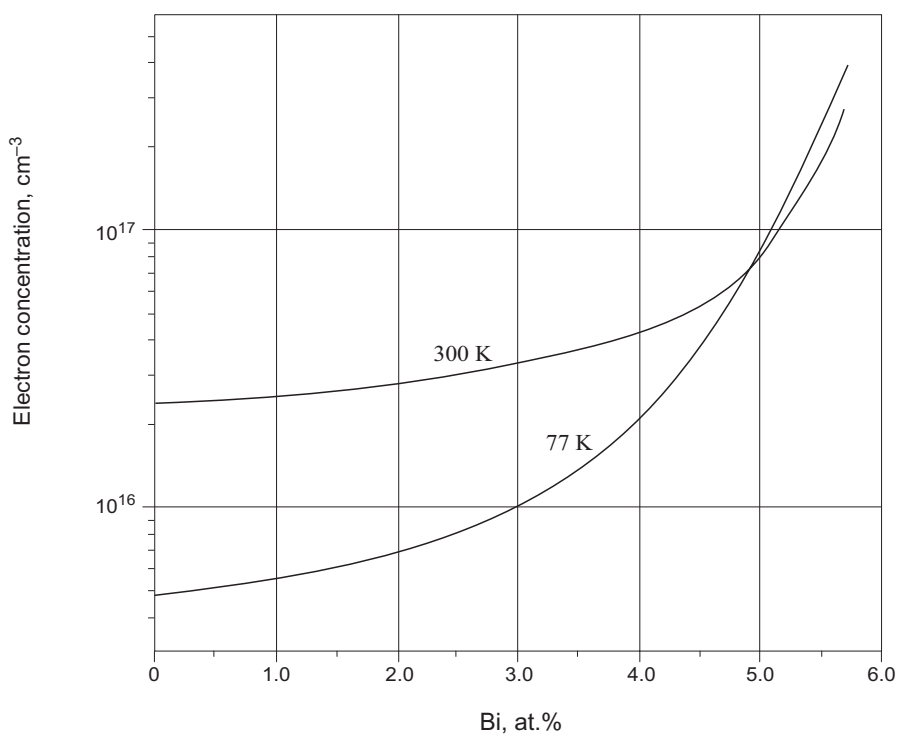


Fig. 17: Bi-In-Sb.
Electron mobility of
 $\text{InSb}_{1-x}\text{Bi}_x$ vs Bi
concentration at 77
and 300 K

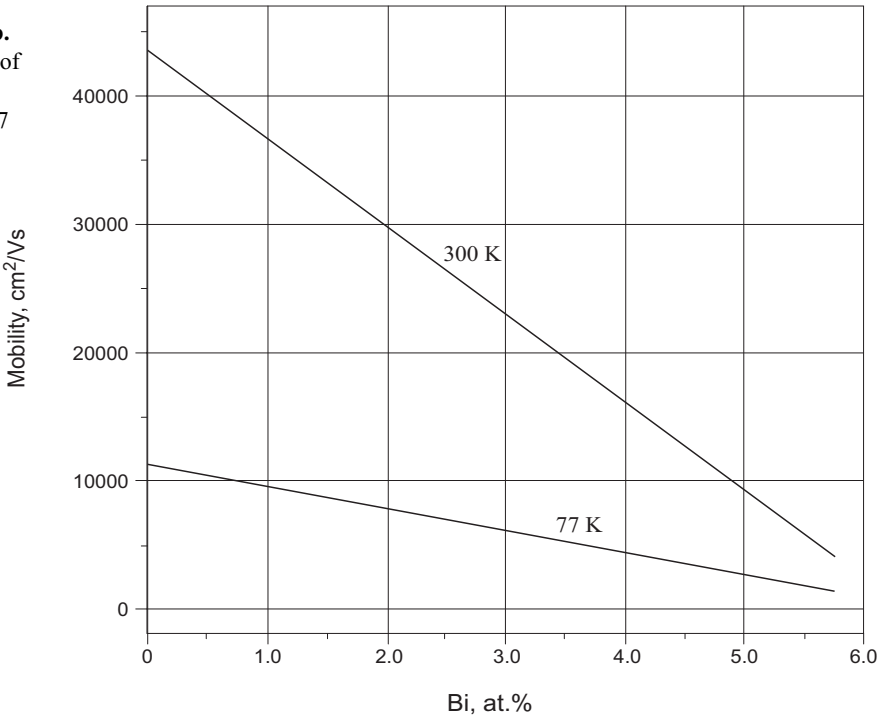


Fig. 18: Bi-In-Sb.
Metastable phase map
of (110) oriented
 $\text{InSb}_{1-x}\text{Bi}_x$ films as a
function of
composition and
annealing
temperature

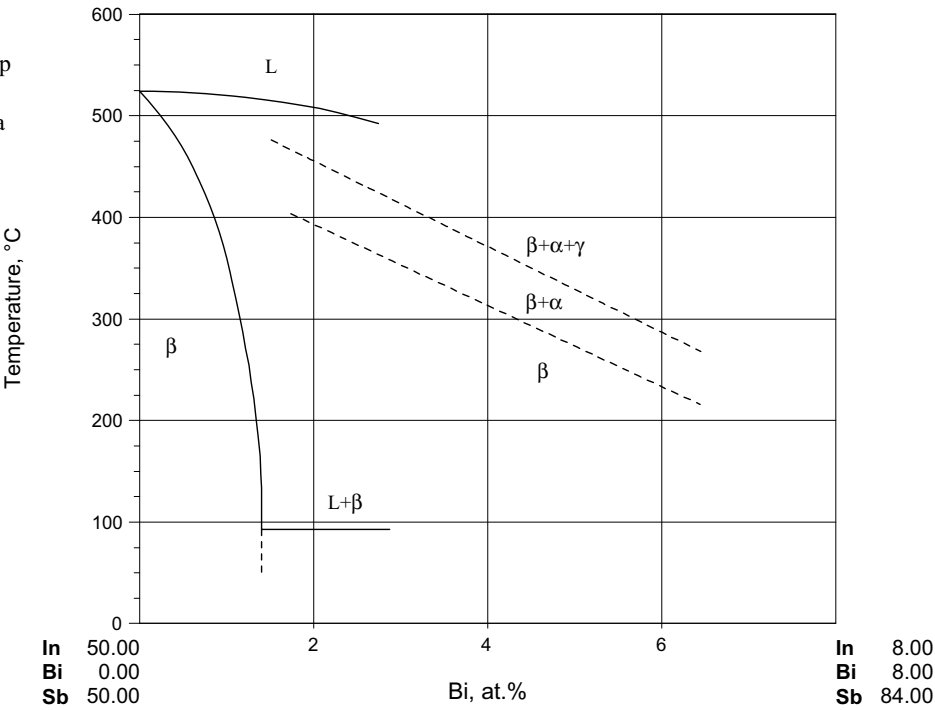


Fig. 19a: Bi-In-Sb.
Composition
dependence of the
band gap E_G at 0 (a),
77 (b) and 300 K (c)
in $\text{InSb}_{1-x}\text{Bi}_x$ solid
solutions

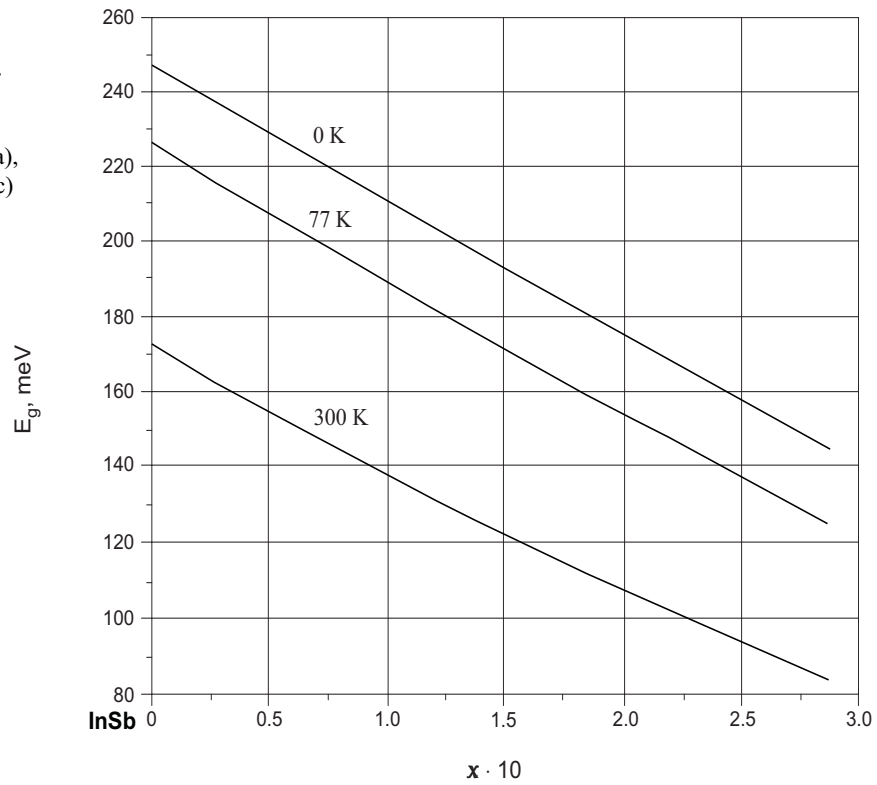


Fig. 19b: Bi-In-Sb.
Composition
dependence of the
band gap temperature
coefficient
($\gamma = -\Delta E_G / \Delta t$)
of $\text{InSb}_{1-x}\text{Bi}_x$ solid
solutions

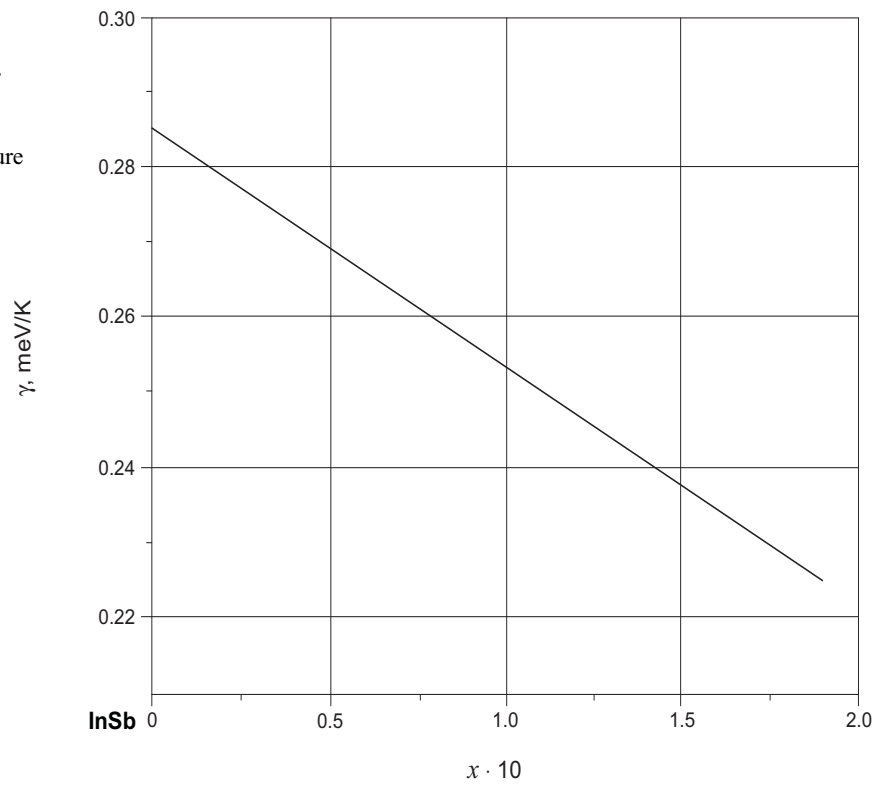


Fig. 20: Bi-In-Sb.

Composition dependence of microhardness of $\text{InSb}_{1-x}\text{Bi}_x$ solid solutions along the InSb-Bi (a), InSb-InBi (b), and InSb-In₂Bi (c) cross sections

